Fuel Processing Technology 141 (2016) 148–158

Contents lists available at ScienceDirect

Fuel Processing Technology

journal homepage: www.elsevier.com/locate/fuproc

Steam–oxygen gasification of forest residues and bark followed by hot gas filtration and catalytic reforming of tars: Results of an extended time test

Esa Kurkela *, Minna Kurkela, Ilkka Hiltunen

VTT Technical Research Centre of Finland Ltd, PO Box 1000, FI-02044 VTT, Finland

ARTICLE INFO

Article history:
Received 2 March 2015
Received in revised form 19 May 2015
Accepted 1 June 2015
Available online 15 June 2015

Keywords:
Biomass
Gasification
Fluidized-bed
Filtration
Reforming

ABSTRACT

Steam–oxygen gasification in a Circulating Fluidized-bed (CFB) reactor was developed for producing transportation fuels from different wood residues. This article presents the results of a two week test campaign, in which crushed forest residues and industrial bark mixture were used as the feedstocks. The aim of the work was to carry out extended time testing of the developed gasification and hot gas cleaning process and to determine the fate of different gas contaminants and trace components of wood. In the test runs, wood fuels were gasified in the CFB reactor at a 0.2–0.25 MPa pressure using a mixture of steam and oxygen as the gasification agent. A mixture of sand and dolomite was used as the bed material in order to maintain stable fluidization and to catalyse in-situ tar decomposition before hot filtration. Raw gas was filtered at ca. 550 °C and the filtered gas was then led into a two-stage catalytic tar reformer. The gasifier performance and the concentrations of different gas contaminants were determined at four different operating variable set points during a total of 215 h of operation. The results for carbon conversion efficiency, raw gas composition and the fate of fuel nitrogen, chlorine and trace metals are presented in this paper. The concentrations of gas contaminants were determined after the ceramic filter unit and after the catalytic reformer. The conversion efficiencies for hydrocarbon gases, tars and ammonia in the reformer are also presented. The test run was carried out as a continuous operation without any interruptions or operational problems.

1. Introduction

Advanced 2nd generation biofuels can be produced from a wide variety of biomass feedstocks utilising many different biotechnical or thermochemical conversion pathways [1]. Gasification-based alternatives have two principal advantages over most other conversion routes. Firstly, a wide variety of biomass qualities as well as many waste streams can be used as feedstock. Secondly, various different end products (e.g., methanol, DME, Fischer Tropsch Diesel and Synthetic Natural Gas) can be produced from a mixture of hydrogen and carbon monoxide (syngas).

Different types of fluidized-bed gasifiers have been industrially applied in power and heat applications already since the 1980s. At present several air-blown CFB gasifiers as well as dual fluidized-bed steam gasifiers operating at atmospheric pressure are in industrial use for example in Finland, Austria and Germany [1–3]. Atmospheric-pressure dual bed steam gasification has also recently been demonstrated in a semi-industrial scale production of Synthetic Natural Gas in Sweden [4].

Pressurised oxygen-blown biomass gasification based on bubbling fluidised-bed reactors was also developed already in the 1980s in Europe and in the USA [5,6], but without commercial breakthrough. In addition, the first industrial scale pressurised fluidized-bed gasification plants using brown coal and peat as the feedstock were operated in Germany and Finland in the late 1980s and early 1990s [7–9]. However, these gasification systems were initially developed for coal and not for biomass feedstocks, which have significantly higher volatile matter content and different ash composition. Very good operation experiences were obtained at the High Temperature Winkler demonstration plant in Germany with Rhenish brown coal [7], whereas the operation with peat at the Oulu ammonia plant in Finland already suffered from problems related to the high tar content of syngas and sintering of the peat ash [8,9]. At the Oulu gasification plant ash sintering problems limited the operation temperature of the gasifier to below 970 °C, resulting in 0.5–1 g/m^3 naphthalene concentrations. This led to deposit formation problems in the final gas cooler and naphthalene condensation in the cooler of the syngas compression system [9]. In addition, ash sintering and melting created deposits in the gas outlet pipe and in the cyclone and blocked the return leg of the recycling cyclone.

Previous studies on pressurised air-blown gasification of coal, peat and wood [10] have shown that tar yields in wood gasification were

* Corresponding author.
E-mail address: esa.kurkela@vtt.fi (E. Kurkela).

http://dx.doi.org/10.1016/j.fuproc.2015.06.005

still almost an order of magnitude higher than those of peat gasification. Furthermore, biomass ash usually has high concentrations of alkali metals and silica, resulting in more problematic ash behaviour than that observed with peat or coal [11]. These previous experiences were taken as a starting point in 2005, when the development of an optimal biomass gasification process for syngas applications was started again in Finland [12]. The target of the development was a process concept for intermediate scale production of transport fuels (fuel production ca. 100 kton/a) with good heat integration to forest industries or other heat-consuming industries [12–15]. The commercialization of CFB gasifiers in the Finnish power and heat market had also created valuable industrial experience and a good technical basis for designing gasifiers for more demanding syngas applications. In 2007–2012, pressurised steam–oxygen-blown Circulating Fluidised Bed (CFB) gasification was intensively developed at VTT [12,16]. The R&D impetus was related to industrial plans for the production of liquid transportation fuels from forest residues. In the developed process, wood feedstocks are first converted into raw gasification gas, also containing high concentrations of tars and hydrocarbon gases. This hot raw gas leaves the gasifier at ca. 900 °C and is cooled to ca. 550 °C and then filtered before catalytic reforming of tars and hydrocarbon gases. After the reformer the product gas is suitable for final gas cleaning and conditioning using industrially proven gas treatment processes such as shift conversion and acid gas removal processes. Economically promising processes have been designed [12,14] on the basis of this concept, with special emphasis on maximising the overall biomass utilisation efficiency by using the by-product heat of the gas cooling and synthesis process, as well as off-gases from the synthesis, for generating heat for process industry or district heating.

Our previous study [16] focused on the initial development of the process concept and described the effects of the gasifier operating pressure, used bed material and other main gasifier operating variables on the gasifier performance. The main focus was on the gasifier operation, whereas the performance of the filter unit and the reformer was not yet studied in detail. In these studies we observed that CFB gasification is a stable and easily controlled process when the gasifier is operated at pressures up to 0.4 MPa, whereas operation above 0.5 MPa is challenging due to overheating of the bottom part of the gasifier bed, resulting in ash sintering problems. At lower gasification pressures, the bed material calcium as well as the inherent wood calcium is in the form of CaO, which has many positive effects on gasification as discussed in more detail in [11,16]. At higher pressures calcium is in the form of $CaCO_3$, which does not have similar positive effects on tar decomposition and ash chemistry. Most of the previous tests were carried out with pelletized wood fuels, which are easier to handle at the test rig, whereas the extended time test of this article was carried out using the most potential Finnish biomass feedstocks in their original physical form, without expensive pelletizing.

This paper presents the results of the extended-time gasification and gas cleaning tests, in which the performances of the gasifier, hot filter unit and the catalytic reformer were determined during a 215-hour test run. The gasification process was operated according to the basic process concept identified in the previous R&D stage [16] to be most reliable from the operation point of view. In this extended-time test run, the gasifier was operated at 0.2–0.25 MPa and at 910 °C, filtration was carried out at ca. 550 °C and the filtered gas was reformed in a two stage reformer, in which three types of catalysts were used in order to achieve stable tar decomposition without soot formation problems. Background studies on hot gas cleaning described in [17] had created the basis for the design of the raw gas cleaning process. The main objective of the extended time test of this article was to demonstrate stable and problem-free operation of the three key unit operations of the process with the two most potential Finnish wood feedstocks, bark and forest residues. In addition, the fates of different gas contaminants in the gasification, filtration and reforming processes were determined in order to create data for the design of the final gas cleaning train before the synthesis processes.

2. Experimental

The 215-hour gasification test run was carried out using three different wood types as the feedstock. Different batches of similar feedstocks had already previously been tested for shorter test periods as described in [16]. Wood pellets of 8 mm diameter (later referred to as P-W) were made in Finland from clean wood sawdust (pine and spruce) and they did not contain any bark. The pellets were crushed to below 5 mm sieve before loading into the gasifier feed hopper. The crushed forest wood residues (FWR) were collected from Eastern Finland and they contained mainly residues from forest thinning from pine and spruce forests. The crushed bark (Bark), which contained 20–30% of stem wood, was a mixture of softwood bark and birch bark and it originated from an industrial pulp and paper mill in Eastern Finland. The forest residues and bark were first dried during the summer in open piles, assisted by warm air blowing. Then the dried material was crushed to below 10 mm sieve. Table 1 presents the proximate and ultimate analyses and elemental ash compositions of the feedstocks as averages for several individual set point samples. Photographs of the feedstocks are presented in Fig. 1. Five representative samples of 3–5 l were taken from each tested feedstock, and then the samples were divided into smaller analytical samples for the different analyses. The results in Table 1 are given as the average of five replicate feedstock samples. The analytical samples and the feedstock analysis results were considered to represent the fuel batches satisfactorily.

A mixture of 70 wt.% dolomite and 30 wt.% sand was used as the bed material in this test run. This bed material mixture was found in previous tests [16] to be a good choice when the gasification pressure was below 0.4 MPa. Dolomite originated from Sweden and was sieved to 0.1–0.6 mm particle sizes. The silica sand material was Finnish and 90 wt.% of the particles were within the range of 0.1–0.4 mm. This sand is also used as a bed material at several industrial gasification and combustion plants in Finland. The chemical composition of the bed materials is given in reference [16].

The tests were carried out using the Process Development Unit called UCG-PDU illustrated in Fig. 2. The figure also shows the sampling points of gas analysis and for collecting different gas contaminant samples. This PDU is based on a pressurised circulating fluidised-bed reactor using steam and oxygen as the primary fluidising agents, which are pre-

Table 1
Feedstock analyses.

Fuel	Bark	FWR	CP-W
LHV, MJ/kg (db)	19.7	19.8	19.2
Moisture, wt.%	12.2	10.5	7.9
Proximate analysis, wt.% (db)			
Volatile matter	77.2	76.3	83.3
Fixed carbon	19.8	21.1	16.3
Ash	3.0	2.6	0.4
Ultimate analysis, wt.% (db)			
C	51.9	51.9	50.7
H	5.9	5.7	5.9
N	0.3	0.4	0.1
S	0.03	0.03	0.01
O (as difference)	38.87	39.37	42.89
Ash	3.0	2.6	0.4
Elemental composition of ash, g/kg dry matter of ash			
Si	34	90	17
Al	13	12	4.0
Fe	9.0	8.0	48
Ca	265	215	380
Mg	32	28	17
K	67	68	90
Na	3.6	3.4	–
Ti	0.6	0.7	–
S	7.9	10	14
P	18	22	11

db: dry basis.

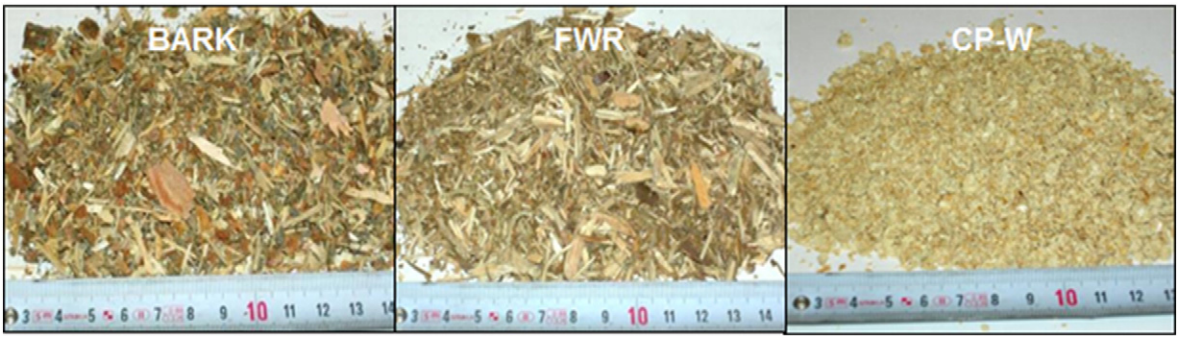

Fig. 1. Photographs of the feedstocks.

mixed and fed below the distributor plate. Air can also be used as the fluidising gas and a small amount of air was also fed at the steam–oxygen gasification set points of this paper for safety reasons in order to be able to shift rapidly from oxygen-blown to air-blown operation in the case of possible operational challenges concerning steam or fuel feeding. In this test run all the gasification agents were introduced as primary fluidization gas and no secondary feeding of O_2/steam/air was used. The fuel and bed material mixture was fed into the gasifier at 185 cm above the distributor plate just below the conical section, where the gasifier diameter was enlarged.

The gasifier and the filter unit are described in more detail in [16]. The inner diameter of the gasifier is 102 mm in the bed section and 152 mm in the upper part of the gasifier tube. The gasifier height from the fluidizing gas distributor to the gas outlet pipe is 8.7 m. The gasifier, the recycling cyclone and the return leg are all well insulated and mounted into a large 11 metre high pressure vessel. The heat losses are minimized by using electrical heaters around the gasifier tube and the cyclone. The heaters are divided into four vertical blocks and each heating block is controlled so that the temperature of the heater is set to 5–10 °C lower than the temperature measured from inside the gasifier tube. The heating elements and the inner reactors are also well insulated by heat-resistant ceramic wool. This heating and insulation arrangement aimed at as close to adiabatic operation as possible, and in practice the heat losses calculated from the material and energy balances were in the range of only 5–10%. Gasification temperatures were measured by K-type thermocouples. The "bed temperature" was calculated as an average of the readings of three thermocouples located at 20, 60 and 110 cm above the distributor plate. The "upper part temperature" was defined as the average of the readings of five thermocouples, which were located 2.9, 3.9, 5.9, 8.2 and 8.7 m above the distributor plate.

The produced gas flows up to the top of the reactor, where the entrained bed material together with ash and unconverted feedstock are separated from the gas in a recycle cyclone and returned back to the bottom of the reactor. After the cyclone separator, the gas is cooled down to 530–560 °C and routed to a filtration unit where dust and condensed alkali and heavy metals are separated using ceramic candle filters. The filter was designed by VTT according to experience obtained

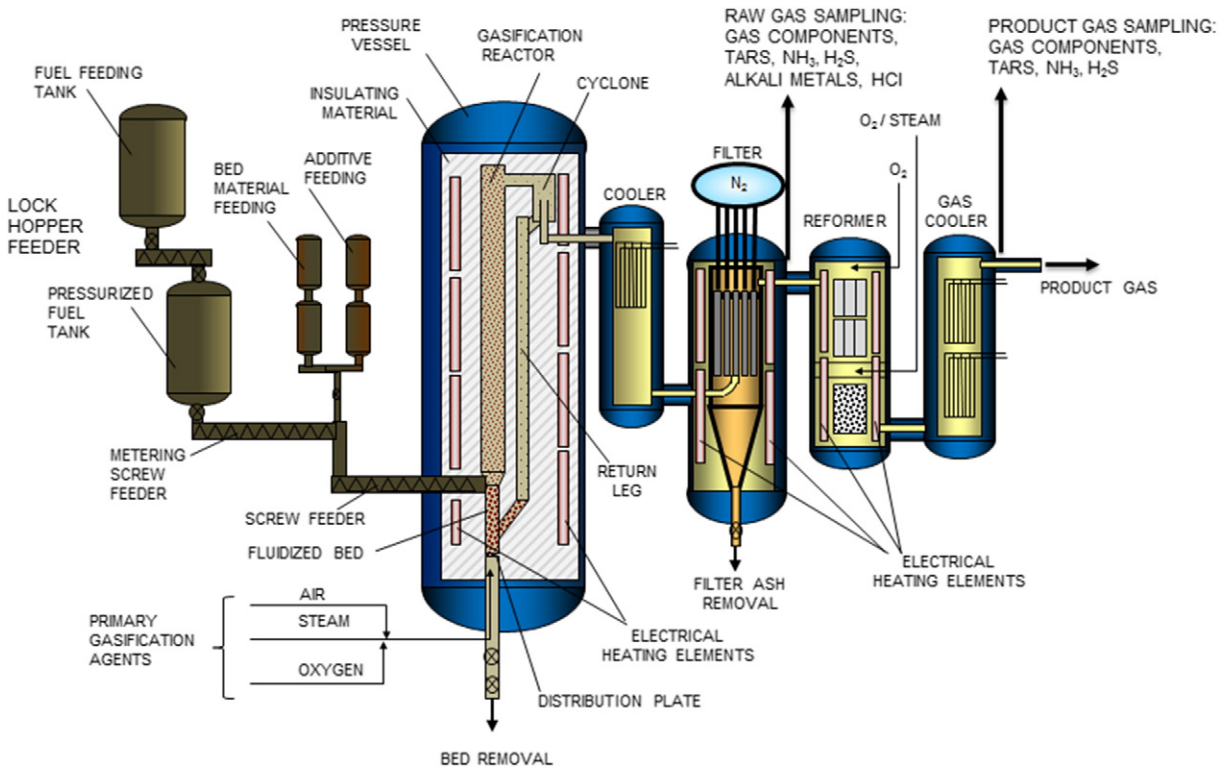

Fig. 2. VTT's test rig for steam–oxygen blown gasification of biomass.

in IGCC-related projects realised in the 1990s [17,18]. The filter consisted of 12 one-metre filter elements, which were organised in four pulse-cleaning clusters. Filter elements were mounted on a thick metal tube sheet using an appropriate gasket material to avoid leakages. The filter was designed for a face velocity of 1.5–2 cm/s. Relatively high filtration surface area was needed due to the fact that the particle size and density of the char particles are rather low [17]. Dust cake was removed by using rapid cleaning pulses. One cluster of three elements was pulsed at a time, and pulse cleaning intervals were controlled so that stable pressure drop variation was achieved for a given gas flow rate. In this test run rigid candle filters (Pall Schumalith®) were used as filter elements.

After the separation of dust in the filtration unit, gas was introduced into a multi-stage catalytic reforming unit operated autothermally with oxygen and steam. In the reformer, the tars and hydrocarbons were catalytically reformed to carbon monoxide and hydrogen at elevated temperatures in the range of 850–990 °C. Different reformer designs were developed and tested during the six-year R&D programme. The concept applied in the test run of this paper, illustrated in Fig. 3, is based on the invented method for avoiding the well-known soot formation problems [17,19,20] of tar reforming by using a staged reformer concept as described in [21,22]. In the pre-reformer, heavy tars and C_2-hydrocarbons are decomposed and the gas temperature is gradually increased from the filtration temperature up to 800–850 °C, which is reached by the end of the pre-reformer (T_2 in Fig. 3). This partially cleaned gas then flows through the final reformer, in which most of the tars and benzene are decomposed and part of the methane is reformed. A mixture of steam and oxygen is also fed into the final reformer in order to achieve target operation temperatures. The steam feed rate into the final reformer was kept constant, while the oxygen feed was controlled so that the target reformer temperatures were achieved. The oxygen feed was controlled primarily by reformer outlet temperature, but it was also restricted by the permitted maximum temperature of the catalyst bed, which was usually measured close to the top surface of the final reformer bed. In this test run, the pre-reformer was constructed using monolith-type catalyst elements with two different compositions. The first layer included VTT's proprietary zirconia catalyst, which acts as a selective oxidation catalyst for heavy tars, and the second element contained a noble metal catalyst supplied by a commercial catalyst manufacturer. This second element was needed to fully decompose C_2-hydrocarbons before entering into the final reformer, as described in [21]. The final reformer was a fixed-bed reactor in which nickel-based steam reforming catalysts were used.

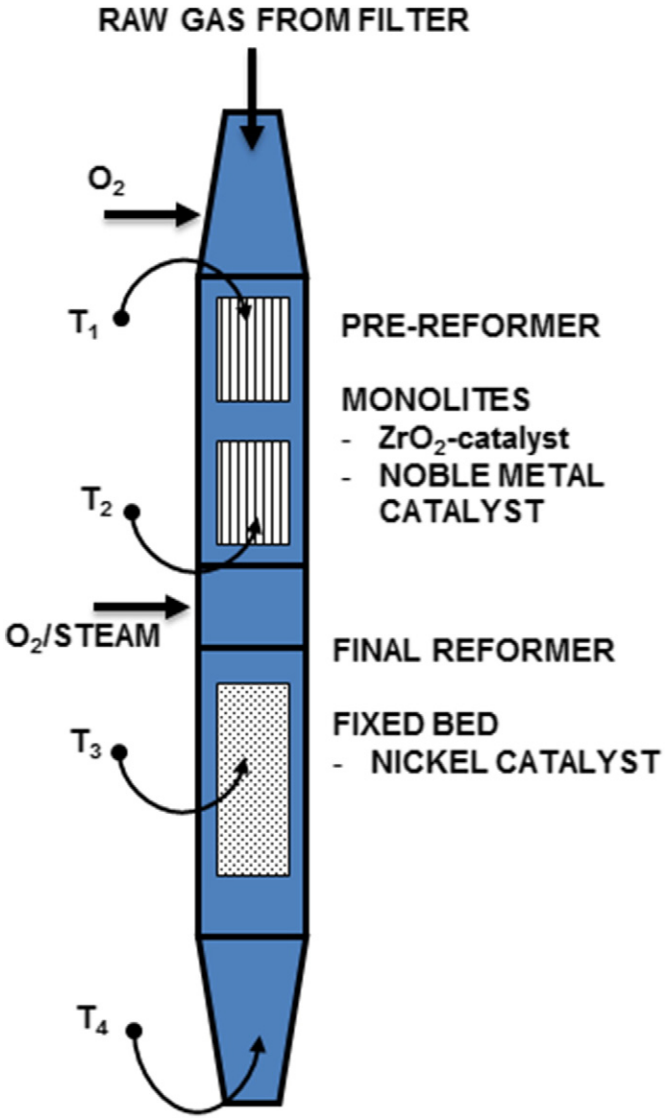

Fig. 3. Staged reformer concept used in the extended time test run.

The gas composition was measured from two process points. The raw gas sampling point was located in between the filter unit and the reformer (Fig. 2). The second sampling point was after the reformer and the final gas cooler. The main gas composition (CO, H_2, CH4 and CO_2) from both process points was monitored by on-line analysers, which were used for process monitoring and control. The data presented in this paper, however, are based on more accurate GC-analyses. The GC analyses were automatically made from the continuously flowing sample gas stream once an hour. The design and operating principles of the sampling lines as well as the used gas analysing methods are described in detail in [18]. The concentrations of volatile organic compounds from benzene to higher molecular weight components up to pyrene were sampled and analysed basically as described in our previous publications [10,16,18], following the European tar protocol [23]. Tar sampling points were located after the hot filter unit before the reformer (Fig. 2) and in the final product gas line after the reformer and clean gas cooler. The gas temperature after the cooler was 250 °C. Nitrogen compounds (NH_3 and HCN) were sampled and analysed by wet chemical methods described in [18,24,25]. The sampling points were the same as those for tar compounds. The H_2S and COS contents of the raw gas and reformed gas were analysed by collecting the gas into 10 dm^3 Teflon bags. The gas in the bags was analysed immediately after sampling using an HP 5890 gas chromatograph equipped with a J&W, GSQ (30 m · 0.53 mm ID, 40 pm + TRAP) column with FPD (HP 19256A). The concentrations of vapour phase alkali metals and chlorine were determined with specially designed extractive sampling methods described in detail in [18]. The sampling point for alkali metals and chlorine was located after the filter unit.

3. Results and discussion

3.1. Gasifier performance

The test run was carried out as a continuous 12-day operation. After the pre-heating and start-up period the plant was operated under gasification conditions continuously for 215 h until the planned shutdown procedure was started. There were no interruptions in the operation, or major process-related problems. Twice during the operation, however, the gasifier had to be switched from oxygen-blown operation to air gasification and then back to O_2/steam blown mode. This was due to problems in safety-related mass flow measurements of steam flow, which stopped the oxygen feed for short periods. In addition, one 10-hour set point was deliberately carried out as air-blown gasification. Total operation time in the steam-oxygen mode was ca. 190 h.

The gasifier was started by a preheating and stabilizing period, carried out with crushed wood pellets, which are homogenous and easy

to feed into the gasifier. Then, several periods with constant operating conditions were completed using bark and forest wood residues. Finally, at the end of the test run the feedstock was switched back to crushed pellets. During the test run a total of 820 kg of crushed pellets, 3920 kg of bark and 3190 kg of forest residues were fed into the gasifier. Representative operational data for the selected set points carried out with crushed bark (Bark), crushed forest wood residues (FWR) and crushed wood pellets (CP-W) are presented in Table 2. The four set points selected for this paper were all carried out at a 0.2 MPa pressure. This pressure level was selected, instead of 0.4 MPa, due to practical reasons related to the use of low bulk density wood fuels. At this pressure the gasifier capacity was relatively low, resulting in reasonable loading intervals of the wood feeding lock hopper system even with a fuel having a bulk density of only ca. 120 kg/m^3.

The temperature of the upper part of the gasifier was kept close to the targeted 910 °C. Fig. 4 shows selected gasifier reactor temperatures during the 45 operating hours of set point A. Two bed temperatures are shown representing the bottom and top parts of the bed (20 cm and 110 cm above the distributor plate), and two temperatures from the upper part of the gasifier (at 5.9 and 8.7 m above the distributor). During this test period the feed rates of gasification agents were kept constant and the small variation in reactor temperatures was due to small changes in feedstock composition and actual fuel feed rate. The highest temperature was usually measured at the top of the bed section, while the temperature at the bottom of the bed was 10–20 °C lower. This was evidently due to the fact that the bed was mainly composed of inert sand and dolomite particles and the amount of charcoal particles was small, which could also be seen in the very low carbon contents of the bottom ash samples. Thus, part of the fluidization oxygen penetrated through the bottom bed and reacted with pyrolysis gases formed from fresh wood particles. This difference in bed temperatures may also have been caused by the small reactor diameter, which decreased the quality of fluidization in the lower dense bed section. In other test runs carried out with uncrushed wood pellets [16], the highest temperatures were usually observed at the bottom of the bed, as the charcoal content of the bed was higher than that in the present test runs carried out with fine crushed wood materials.

Table 2
Operational data for the selected set points with different wood feedstocks.

Set point	A	B	C	D
Gasifier feedstock	Bark	FWR	FWR	CP-W
Moisture content, wt.%	12.2	10.5	10.5	7.9
Fuel feed rate, g/s	10.4	9.1	9.6	11.3
Bed material feed rate, g/s	0.6	0.6	0.7	0.6
Bed material	Dol + S	Dol + S	Dol + S	Dol + S
Primary air, g/s	0.5	0.4	0.4	0.6
Primary steam, g/s	5.3	5.7	5.8	5.8
Primary oxygen, g/s	4.4	4.0	4.0	4.0
Purge nitrogen feed, g/s	1.6	1.5	1.5	1.4
Steam-to-fuel, kg/kg-daf	0.6	0.7	0.7	0.6
O_2 feed, % of stoich. combustion	33.6	35.0	33.0	28.6
O_2 feed, wt.% of gasifier feed gases	44.3	40.5	40.1	39.8
Average gasifier bed-T, °C	923	927	927	920
Average gasifier upper part T, °C	908	907	911	909
P-freeboard, MPa (abs)	0.2	0.2	0.2	0.2
T-filter, °C	526	553	552	558
Filter Pd, mbar	14.3	16.8	16.5	15.2
Dust in filter inlet, g/m^{3}n	10.2	13.8	12.8	11.8
Filter face velocity, cm/s	1.7	1.6	1.7	1.8
Bottom ash, g/s	0.44	0.48	0.46	0.25
Bottom ash, ash content, wt.%	99.4	99.5	99.3	99.4
Filter dust, g/s	0.21	0.27	0.27	0.27
Filter dust, C content, wt.%	24.3	24.8	22.9	23.2
Dry gas, measured				
CO, vol%	18.5	17.4	17.3	18.6
CO_2, vol%	33.5	34.3	34.6	34.1
H_2, vol%	29.7	30.9	30.8	31.3
N_2 (calc. as difference), vol%	10.1	9.4	9.6	7.6
CH_4, vol%	6.9	6.7	6.6	7.2
C_2H_2, vol%	0.01	0.01	0.01	0
C_2H_4, vol%	0.99	0.95	0.87	0.90
C_2H_6, vol%	0.10	0.15	0.11	0.13
C3–C5, vol%	0[a]	0[a]	0[a]	0[a]
H_2S, ppmv	100	172	nd	nd
COS, ppmv	1.9	3.9	nd	nd
Ammonia, ppmv	2730	4970	3060	nd
HCN, ppmv	10.1	16.4	16.4	nd
Sum of tars and benzene in dry gas, g/m^{3}n	19.1	19.3	17.5	17.8
Fluidising velocity, m/s	2.7	2.7	2.7	2.8
Gas velocity at riser top, m/s	2.5	2.3	2.5	2.7
Gas residence time at riser top, s	2.77	3.01	2.85	2.6
Wet gas flow rate, g/s	21.6	19.7	20.8	23.0
H_2O content in wet gas, vol%	35.5	37.6	36.7	33.8
C conversion to gas and tar, %	99.0	98.4	98.6	98.8
K-shift from wet gas composition	0.97	1.00	1.06	1.12
K-shift (calc. at average gasifier upper part T)	0.74	0.75	0.74	0.74
Equilibrium temperature of K-shift	822	810	797	782
Oxygen balance closure, out/in	0.99	0.96	0.99	1.02
Ash balance closure, out/in	0.78	1.04	0.88	0.89

nd = not determined.
[a] Below detection limit of 0.01 vol.%.

The fluidization velocities presented in Table 2 were calculated on the basis of the fluidising gas feed rates, actual temperature and pressure at the bottom of the bed, and the empty reactor tube diameter. The velocity at the top of the gasifier, also presented in Table 2, was calculated on the basis of the actual pressure and temperature of the gasifier top, the upper part reactor diameter and using the raw gas flow rate calculated from material balances. The diameters of the bed and the upper part of the gasifier were designed so that the gas velocity at the gasifier top is almost the same as the fluidizing velocity at the bottom of the bed. The highest gas velocities in the reactor occur at the top of the bed section just before the conical enlargement section, due to gas evolution from the gasification reactions taking place in the bed. The share of O_2 in the steam–oxygen mixture used as the fluidising gas was 40–44 wt.%. A mixture of 30 wt.% sand and 70 wt.% dolomite was used at all set points as the bed material. Under these operating conditions, the CO_2 partial pressure of product gas was low enough so that the bed material calcium was calcined to CaO throughout the reactor height. No operational problems were encountered in these tests and the gasifier performance was rather similar with all tested fuel types. After the test run the reactor was opened and it was observed that the gasifier tube, cyclone and return leg were clean and there were no signs of ash deposits. The bottom ash samples did not contain significantly sintered ash particles.

The previously reported [16] parametric studies already demonstrated that high carbon conversion efficiencies can be achieved in steam–oxygen blown CFB gasification with fine-grained biomass fuel. This was described to be partly due to more oxidative conditions in the lower part of the gasifier, where the charcoal particles from the recycle flow meet fresh oxygen and steam [16] as the wood pyrolysis takes place mainly in the upper part of the gasifier. Consequently, the conversion of charcoal particles is not only dependent on char gasification reactions, which are strongly inhibited by CO and H_2 and are an order of magnitude slower than oxidation reactions [16]. The results of the 215-hour extended-time test clearly proved that these conclusions were also valid during longer test periods, in which the ash and charcoal inventory of the gasifier certainly reached a steady state. The carbon losses at the set points of this paper were only 1–1.6%. The bottom ash did not contain any carbon and the carbon content of filter fines was also relatively low, in the range of 23–25 wt.%. The carbon conversions presented in Table 2 were calculated indirectly on the basis of wood carbon input during the whole set point period and the analysed carbon contents and determined weights of filter and bottom ash streams.

The results for dry gas analysis and the concentrations of water vapour in wet gas are also presented in Table 2. It can be seen that the hydrogen contents in dry gas were already rather high in the raw gas before reforming. The equilibrium constant of the water gas shift reaction (K-shift) calculated from the wet gas analysis is also presented in

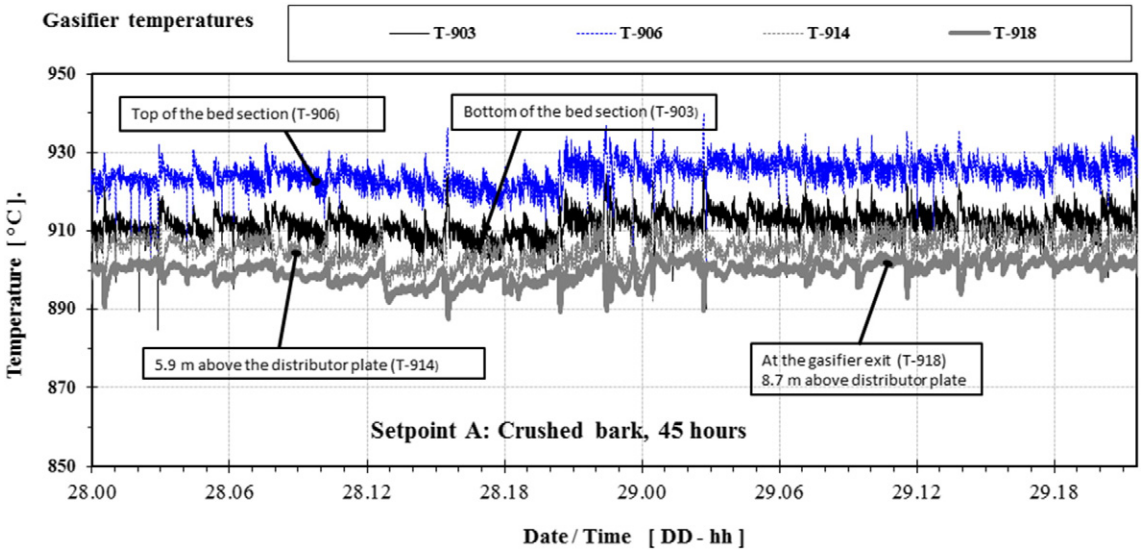

Fig. 4. Selected gasifier reactor temperatures at set point A.

Table 2. This measured K-value can be compared to the equilibrium K-value calculated at the average gasifier upper part temperature using the equation given by Rhinehart et al. [26]. In addition, Table 2 also shows the equilibrium temperature which would give the K-value corresponding to the measured gas composition. It should be mentioned that the sampling point of gas analysis was located after the ceramic filter unit, where the process temperature was ca. 500 °C. Comparison of the K-value data shown in Table 2 indicates that the water gas shift reaction was still continuing in the cyclone and in the upper part of the gas cooler, and the gas composition corresponded to the equilibrium calculated at 780–820 °C. Methane and C_2H_4 were the most significant hydrocarbon gases, with lower concentrations of C_2H_2 and C_2H_6. The concentrations of C_3–C_5 hydrocarbon gases were below the detection limit of the used gas chromatographic analysis method (<0.01%).

Elemental material balances were calculated from the average measuring data for each set point in a way similar to that described in our previous air-blown gasification tests [10,18]. However, in oxygen–blown gasification the nitrogen balance could not be used for calculating the dry gas flow rate due to the low input of nitrogen and due to the fact that part of the purge nitrogen, which was fed into the fuel feeding lock-hoppers and ash removal hoppers, evidently did not enter into the product gas but escaped from the hoppers during pressurising and depressurising cycles. Neither was it possible to accurately measure the flow rate of hot raw gas containing tar. Consequently, the elemental carbon balance was used to calculate the dry gas flow rate. Hydrogen balance was similarly used for calculating the water vapour mass flow. In this method the inaccuracies of all measurements and of the material balance calculation accumulate in the oxygen balance. At these set points the oxygen balance closure was reasonably good. The ash balances were directly calculated from output and input figures using the average analyses and weighed amounts of wood and bed material as the input and the analyses and weighing results of the bottom ash and filter fines as the output. Despite the long set points and careful analyses, the ash balance closures were not fully satisfactory. This is at least partly due to the low ash content of wood fuels, and similar inaccuracies have also been reported in previous experiments [11,27,28].

Measured concentrations of different tar components are presented in Table 3. In addition to the individual concentrations, the sum of light tars (from Pyridine to Cresol) and the sum of PAC compounds heavier than naphthalene are presented. Total tar concentration in the dry gas was in the range of 4.8–5.7 g/m^{3}n and that of benzene varied in the

Table 3
GC tar analyses for the set points.

Set point	A	B	C	D
Fuel	Bark	FWR	FWR	CP-W
Concentration, mg/m^{3}n in dry gas				
Benzene	13,757	13,605	12,733	12,806
Pyridine	27	65	38	7
1H-Pyrrole	0	0	0	0
Toluene	200	212	165	160
Ethenylbenzene	33	41	32	20
m-Xylene	0	0	0	0
Ethynylbenzene	2	1	1	1
Styrene	119	113	90	112
o-Xylene	0	0	0	0
Benzaldehyde	0	0	0	0
Phenol	10	12	10	10
Benzonitrile	0	0	0	0
4-Methylstyrene	0	0	0	0
Indene	111	144	108	110
o-Cresol	0	0	0	0
m+p-Cresol	0	0	0	0
Naphthalene	3304	3376	2942	3089
Quinoline	0	8	3	0
Isoquinoline	0	0	0	0
1H-Indole	0	0	0	0
2-Methylnaphthalene	23	25	20	20
1-Methylnaphthalene	15	17	14	14
Biphenyl	74	76	62	65
2-Ethylnaphthalene	16	15	11	9
Acenaphthylene	298	377	302	363
Acenaphthene	199	199	162	132
Dibenzofurane	12	25	18	19
Bibenzyl	0	0	0	0
2-Methyl-1-Naphthol	9	12	9	10
Fluorene	30	44	30	33
Phenanthere	492	541	444	472
Anthracene	81	100	79	84
4H-Cyclopenta(def)Phenantherene	8	12	9	10
Fluoranthene	129	169	132	153
Benz(e)acenaphthylene	12	17	13	18
Pyrene	108	133	102	124
Sum of tars	5312	5735	4796	5034
Sum of tars and benzene	19,069	19,340	17,529	17,840
Benzene	13,757	13,605	12,733	12,806
Light tars	502	589	445	419
Naphthalene	3304	3376	2942	3089
Heavier PAC	1506	1770	1409	1525

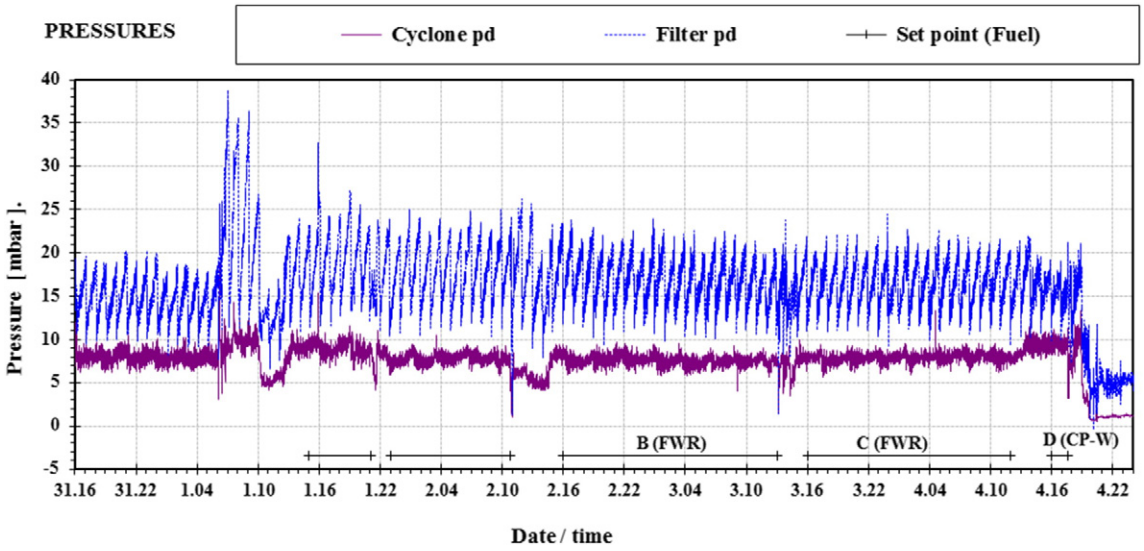

Fig. 5. Pressure drop of the filter and recycling cyclone during the last 90 h of the test run.

range of 12.7–13.8 g/m^{3}n. The concentrations of light tars were low, as could be expected due to the high operation temperature. The concentrations of heavier PACs were also rather low compared to the results of some less successful test periods of our earlier test runs described in [11,16]. The results with all three tested feedstocks were of the same order of magnitude with no clear differences, which can be explained by the strong catalysing effects of calcium oxide in the bed material.

The concentrations of ammonia and hydrogen cyanide were measured at set points A, B and C. The results of the extended time tests appeared to be in good agreement with those of the previously presented steam–oxygen blown tests [16] and of earlier air-blown bubbling and circulating fluidised-bed tests [24,25,27]. Most of the wood nitrogen was converted to ammonia, the calculated conversions being 85.4%, 105% and 72.9% for set points A, B and C, respectively. Over 100% conversion at set point B indicates that the wood nitrogen content during the ammonia sampling period was higher than the average N content used in the material balance calculations. Conversions to HCN were very low, representing less than 0.5% of the wood nitrogen. The H_2S content of product gas after the filter unit was 100 ppmv (in dry gas) at set point A and 172 ppmv (in dry gas) at set point B. COS concentrations were 2 ppmv and 4 ppmv, respectively. No traces of organic sulphur components were detected in these gasification tests, which were carried out at relatively high operating temperatures.

3.2. Filtration and fate of trace metals

The most significant challenges facing biomass-derived gas filtration are related to the behaviour of tars in filtration, as is discussed in [17,28,29]. The possible filtration temperature window, typically 350–600 °C, must be defined by the tar load in the gas. At low filtration temperatures, tars may condense in the dust cake or inside the filter pores, leading to stickiness of dust and blocking of the filter pores [17]. On the other hand, too high temperatures (above 600 °C) have been found to result in a rapidly increasing filter pressure drop caused by the thermal soot formation reactions of tars, which in some test runs of air-blown gasification blocked the filter unit completely in less than 5 h [29]. The dust concentration and quality also have clear effects on the filter operability, as described in [16]. The most difficult situation occurs when the dust content is low and the concentration of heavy tars is high.

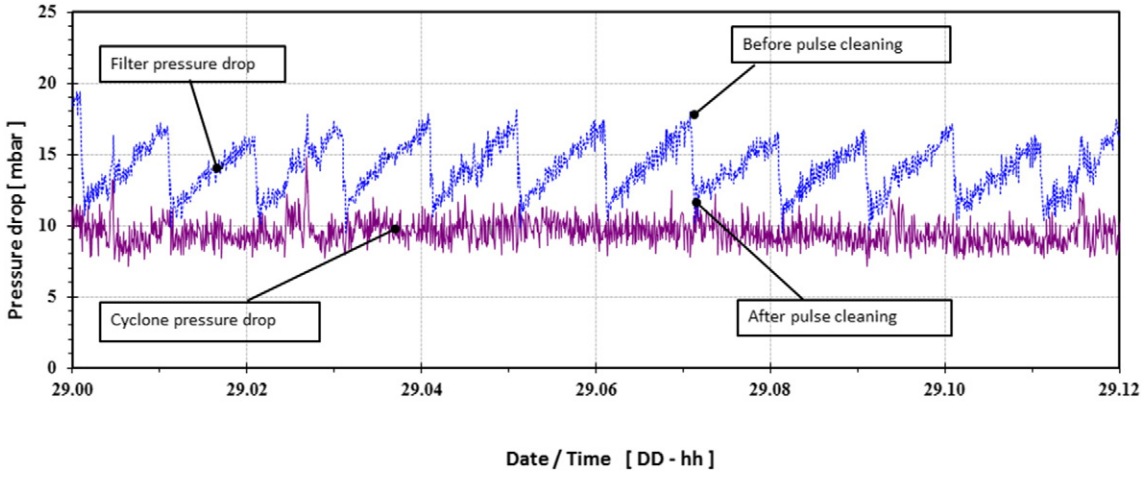

Fig. 6. Filter pressure drop curve for a 12 hour time period, showing the effect of pulse cleaning at set point A.

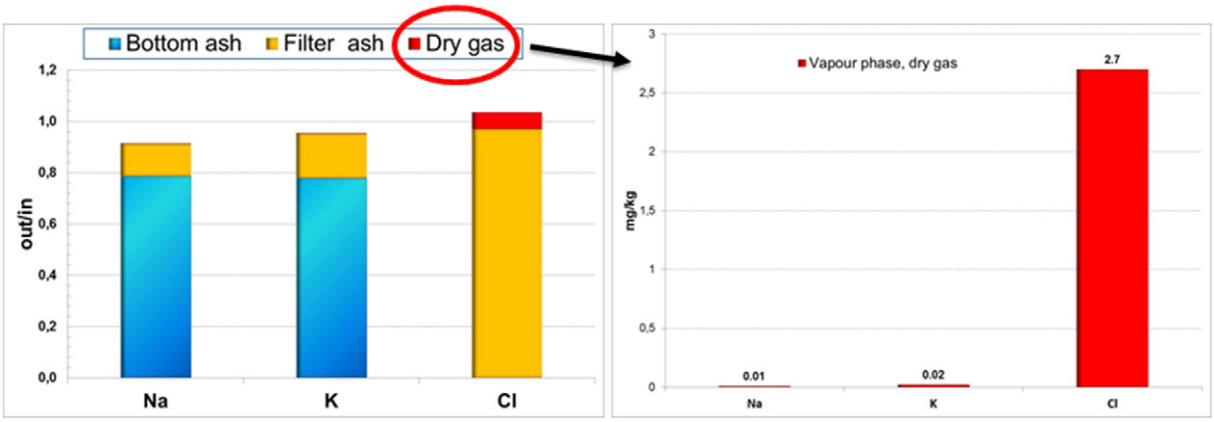

Fig. 7. The measured vapour phase concentration in raw gas and material balances of alkali metals and chlorine at set point C carried out with forest wood residues.

Based on these previous experiences, the filtration temperature was controlled by the gas cooler to a temperature window of 500–560 °C. The dust load in the filter inlet was also at a satisfactory level of 10–14 g/m^{3}n. Stable and unproblematic filter operation was achieved throughout this 215-hour test run, as was expected on the basis of the initial process development phase as described in [16], in which we concluded that stable filtration was achieved in all tests runs when the gasification was realised at or below 0.4 MPa using calcium-based bed materials. Fig. 5 shows the measured pressure drops of the recycling cyclone and the filter unit during the last 90 h of the test run. Both pressure drops showed a similar dependence on changes in the gas flow rate, and there were no indications of increasing filter pressure drop. The filter pressure drop for a 12-hour time period during set point A is illustrated in Fig. 6. The filter elements were pulse cleaned at one hour intervals in order to remove dust cake from the candle filter surfaces. The pulse cleaning interval was set on the basis of the dust loading indicated by the pressure drop curve. This figure illustrates that the baseline pressure drop of the filter immediately after pulse cleaning remains stable, which indicates effective pulse cleaning and unproblematic removal of dust cake. The baseline pressure drop measured at this first set point (10–12 mbar) remained constant throughout the 215-hour test run.

In the low pressure operation of this test run (0.2–0.25 MPa), the bed material dolomite or limestone was efficiently attrited in the gasifier during calcination and during the recycling loop, and the fine calcined dolomite particles appeared to protect the filter cake from sticky particles containing tar and soot. The use of a bed mixture of hard sand particles and more easily grinding and pulverized dolomite particles also helps in binding finely dispersed and partly volatilised wood potassium into the fine and porous dolomite particles in the gasifier as well as on the filter cake, which was also observed in our previous air gasification studies [11].

The role of the filter unit in this gasification process concept is to protect the reformer from dust deposits and alkali attack. This is especially important for the final reformer, which is of fixed-bed design. Throughout this test run the filter was operating practically as total filtration, and no particles were found from the filtered gas when standard sampling systems [18] were used (dust concentration below the detection limit of 5 mg/m^{3}n). The concentrations of alkali metals after the filter unit were determined at set point C, realised with forest residues as the feedstock. The measured concentrations were low, being clearly below 0.05 ppm(m) in dry gas. Fig. 7 shows the measured concentrations of sodium, potassium and chlorine as well as the calculated material balances for set point C. At this set point the material balance closure was relatively good. The input in the material balance was determined on the basis of fuel and bed material feed rates and their average contents of Na, K and Cl. The output flow was calculated on the basis of the weighed amounts of bottom ash, and filter fines and their alkali and chlorine analyses. The gas phase mass flow was calculated from the measured concentration and the dry gas flow rate calculated from elemental material balances. A major part of potassium and sodium is already captured into the bottom ash, and the gas phase concentration after filtration is insignificant. Chlorine behaves differently, as the chlorine content of bottom ash is almost negligible and chlorine is mainly captured into the filter cake. The HCl content of the raw gas after the filter unit was 2.7 ppm, representing 6.5% of the input wood chlorine. The potassium/chlorine molar ratio in wood feedstock was rather high, almost 30, and evidently the chlorine was captured as KCl into the filter ash.

The heavy metal contents of the feedstock, bottom ash and filter ash were determined at set points A and C. The results for the feedstock and filter fines are presented in Table 4. The bottom ash samples throughout the whole test period were so inhomogeneous that the variation in the concentrations between individual samples was too high to get any meaningful results. Thus, only the results for the much more homogenous filter fines are presented. The table also shows the calculated shares of trace metals which were found from the filter fines (in weight % of the input). The results are shown only for those elements of which the concentration was above the detection limit of the analytical method. As bark and FWR were both clean, non-contaminated wood-based feedstocks, the heavy metal concentrations were generally low, which also explains why complete material balances could not be determined. However, these results indicate that gas filtration also has an important role in lowering the heavy metal load of the gas entering the reformer. This would be more important if contaminated wood species were used.

Table 4
Heavy metal concentrations of the feedstock and ash streams at set points A and C.

Set point	A	C
Gasifier feedstock	Bark	FWR
Feedstock concentrations, mg/kg		
As	0.07	0.06
Cu	2.6	2.5
Ni	1.3	1.4
Mn	273	298
Zn	80	48
Filter ash concentrations, mg/kg		
As	5.7	5.5
Cu	33	36
Ni	47	47
Mn	6080	6540
Zn	933	781
wt.% of the input found from the filter ash		
As	55	75
Cu	25	35
Ni	62	88
Mn	45	57
Zn	27	46

Table 5
Results of the process measurements for the reformer.

Set point	A	B	C	D
Gasifier feedstock	Bark	FWR	FWR	CP-W
Reformer temperatures, °C				
T1 inlet (monolite I)	513	524	523	524
T2 prereformer outlet (monolite II)	823	840	857	853
T3 final reformer (Ni)	973	988	1004	995
T4 final reformer/outlet	896	907	928	916
Space velocity in final reformer (ntp), h^{-1}	11,400	10,500	11,100	12,200
Space velocity in final reformer (ntp), h^{-1}	4640	4220	4490	5000
Inlet gas flow (wet gas, calculated)	21.6	19.7	20.8	23.0
Oxygen to reformer, g/s	1.7	1.66	1.76	1.93
Steam to reformer, g/s	1.77	1.68	1.91	1.92
Measured dry gas composition after reformer				
CO, vol%	19.8	19.3	19.8	21.96
CO_2, vol%	33.2	34.8	34.9	32.5
H_2, vol%	34.4	34.4	34.9	37.4
N_2 (calc. as difference), vol%	10.1	8.79	8.48	6.90
CH_4, vol%	2.37	2.67	1.91	1.22
C_2–C_5H_y, vol%	0[a]	0[a]	0[a]	0[a]
H_2S, ppmv	93	150	nd	nd
COS, ppmv	4	7	nd	nd
Ammonia, ppmv	1150	1336	1256	nd
HCN, ppmv	10	13	nd	nd
Benzene concentration, mg/m^{3}n in dry gas	485	845	302	64
Sum of tars, mg/m^{3}n in dry gas	59	93	50	30
Wet gas H_2O concentration, %	38.7	42.2	41.9	37.4
K-shift from measured wet gas composition	0.91	0.85	0.85	0.93
K-shift (calc. at reformer outlet T_4)	0.77	0.75	0.76	0.73
Equilibrium temperature of K-shift	842	865	865	835
Calculated conversions in reformer, %				
CH_4	60.4	55.4	67.5	80.2
C_2–C_5H_y	100	100	100	100
Benzene	95.5	93.0	97.3	99.4
Tars	98.7	98.2	98.8	99.3
NH_3	51.1	69.8	54.0	nd
HCN	−8.2	12.5	nd	nd

nd = not determined.
[a] Below detection limit of 0.01 vol.%.

3.3. Catalytic reforming

The raw gasifier gas from an O_2/steam-blown CFB gasifier contains typically 5–10% methane and 1–2% C_2-hydrocarbon gases together with 15–30 g/m^{3}n of benzene and tars [16]. Secondary gasification or reforming of these organic components is an essentially important unit operation of VTT's gasification process. Catalytic tar removal has been studied at VTT already since the 1990s and this background know-how, summarized in [17], was used to design the reforming concept of the present extended-time test run. In the developed process concept, the reforming of tars and light hydrocarbon gases is realised in a staged process based on oxidation and auto-thermal reforming. One of the challenges of reforming biomass-derived gasification gas, especially at elevated pressures, is soot formation on the catalyst resulting from thermal cracking of tars and C_2-hydrocarbon gases. This may lead to rapid coking of the catalyst, which can be seen as a constantly increasing pressure drop and severely decreasing activity.

In this test run the gasifier was operated at optimised conditions so that the raw gas tar and hydrocarbon loading to the reformer was reasonably low. Total tar and benzene concentration in raw gas entering the reformer was in the range of 17.5–19.3 g/m^{3}n and the content of the most difficult heavy polyaromatic compounds was below 2 g/m^{3}n. The extended time test of this paper demonstrated that the catalyst coking problems could be completely avoided when the reformer was designed (Fig. 3) according to the principles described in [17,21,22] and when the gasifier was operated so that initial tar loading was reasonably low. The role of the pre-reformer was to lower the concentrations of heavy polyaromatic compounds and to decompose C_2-hydrocarbon gases. These components were known to create soot formation in the final reforming, especially when nickel catalyst was used [17]. The main operating conditions and results of the reformer at all set points are presented in Table 5. The pressure drop of the reformer remained constant, varying only as a function of the gas flow rate, as can be seen in Fig. 8. The figure shows the pressure drop over the whole reformer during the last 90 h of the extended-time test run.

The conversion efficiencies achieved in the reformer for tars, benzene, methane and ammonia are presented in Fig. 9. Tar conversion was over 98% at all set points and the residual tar contents at set points A, B, C and D were 59 mg/m^{3}n, 93 mg/m^{3}n, 50 mg/m^{3}n and 30 mg/m^{3}n, respectively. Benzene conversions were 93–97% at set points A–C, carried out with bark and forest residues. Benzene conversion was 99.4% at the last set point carried out with clean wood pellets, which have a very low sulphur content. Methane conversion was also clearly higher in the case of wood pellets than that with wood residues and bark containing more sulphur. This is due to the inhibiting effects of sulphur on the activity of the nickel catalyst, which were studied in detail in [30,31]. The effect of feedstock sulphur content on benzene and methane conversion was always clearly noticed when the feedstock was changed from sawdust to wood residues or vice versa. This effect on conversion efficiency was very rapid and immediately followed the changes in H_2S concentration. The effect of feedstock change is illustrated in Fig. 10, in which the feedstock is changed from FWR to wood pellets and the benzene and naphthalene concentrations of the reformed

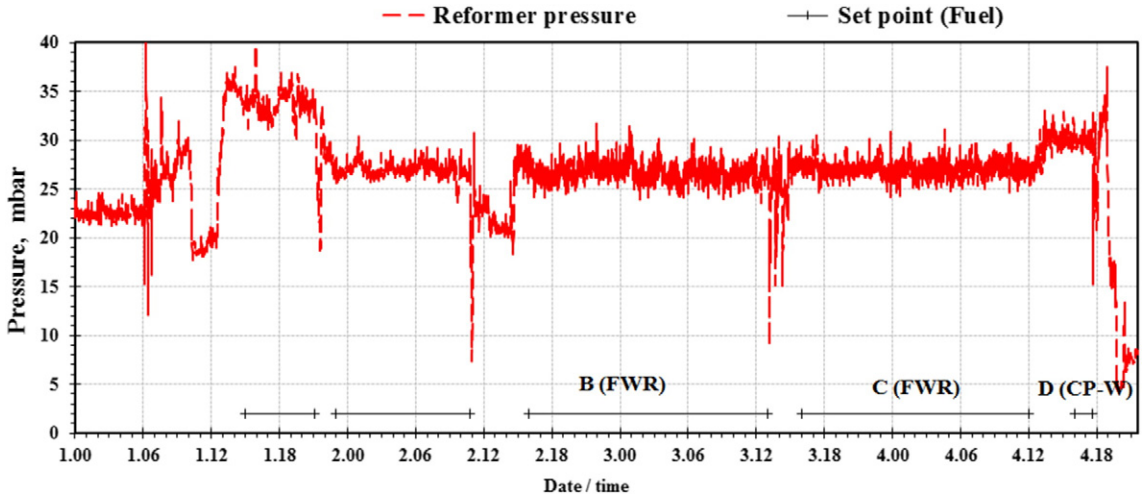

Fig. 8. Reformer pressure drop during the last 90 h of the test run.

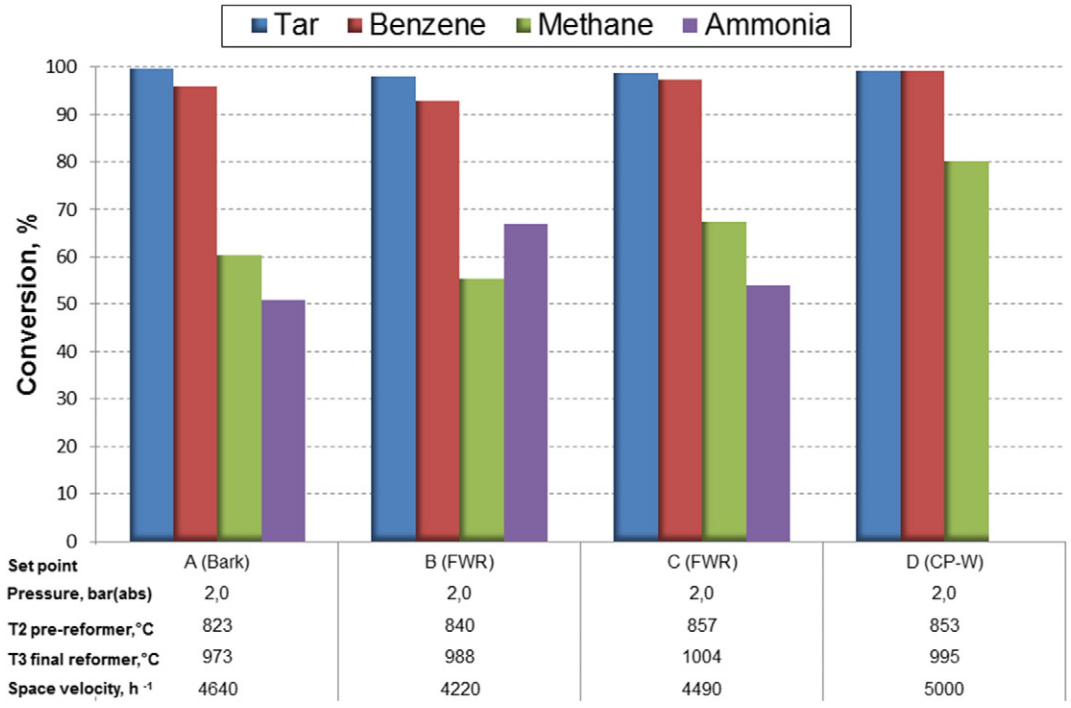

Set point	A (Bark)	B (FWR)	C (FWR)	D (CP-W)
Pressure, bar(abs)	2,0	2,0	2,0	2,0
T2 pre-reformer,°C	823	840	857	853
T3 final reformer,°C	973	988	1004	995
Space velocity, h^{-1}	4640	4220	4490	5000

Fig. 9. Conversion efficiencies in the reformer calculated from measured concentrations and material balances as 100 ∗ (mass flow in − mass flow out) / mass flow in.

gas are measured using a semi-on-line gas chromatographic method. It was typical for the gasification of inhomogeneous forest residues that the feed composition varied cyclically depending on the loading interval of the live-bottom lock hopper of the fuel feeding line. Despite the fact that both the gasification and reforming temperatures were kept constant, the benzene concentration varied with the same frequency as the H_2S content of the gas. After the feedstock was changed to very homogenous and clean wood pellets, the benzene concentration was stabilised at a clearly lower level than with FWR.

The most important result of the test run with respect to reforming was the fact that there were no signs of coking or pressure drop increase. The performance was satisfactory, but could be improved by process optimisation. Some improvements were suggested based on the test data and other experiences of VTT. The efficiency of the pre-reformer could be improved by replacing the monoliths with a fixed-bed pre-reformer. This would also simplify the design of the large industrial scale reformers, as the mounting of a large number of ceramic monoliths into a refractory-lined pressure vessel is a challenging task and it is difficult to avoid some by-pass of gas through the spaces between the monolith elements and the reactor wall. Benzene and methane conversions were not as high as targeted despite relatively high reformer outlet temperatures of 900–930 °C. The performance of the final reformer could be improved by using a more active catalyst, by enlarging the final bed volume and by increasing the average operation temperature of the bed. All these alternatives are being studied in an on-going follow-up project and these results will be published later.

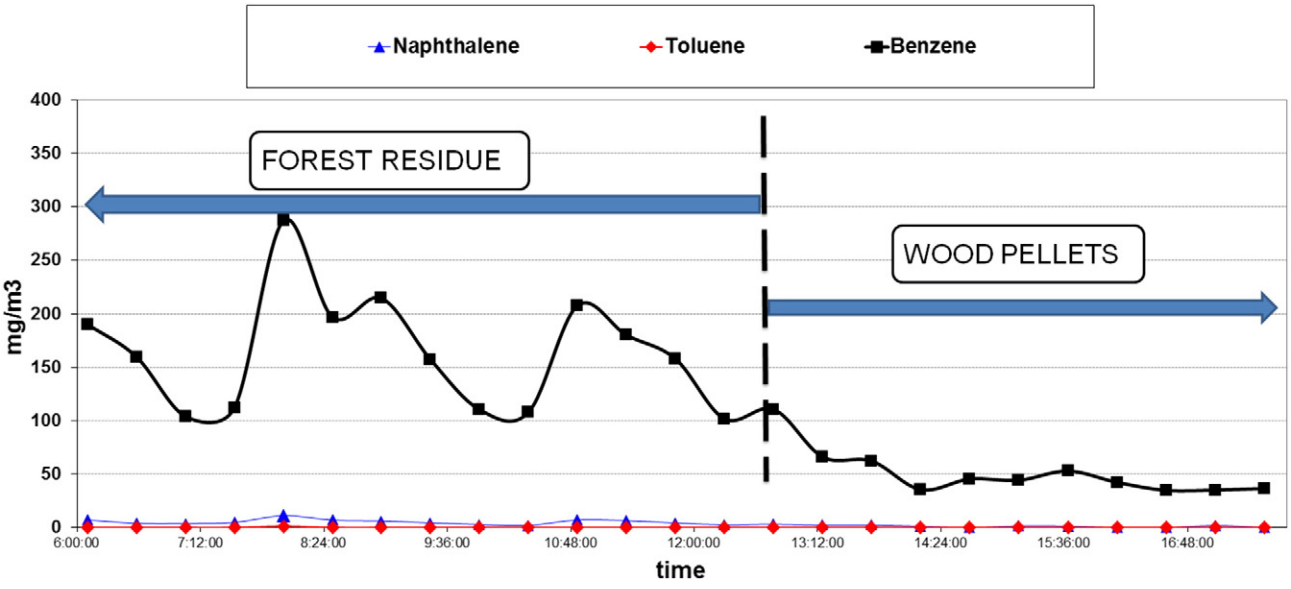

Fig. 10. On-line tar results for the period when feedstock was changed from FWR to clean wood pellets.

4. Conclusions

The 215-hour extended time test was realised as an uninterrupted continuous gasification test run, without any process-related problems. The operation of the gasifier, ceramic filter and the catalytic reformer was smooth and stable set points could be carried out with all three feedstocks: industrial bark mixture, forest wood residues and crushed wood pellets. The test run demonstrated the technical feasibility of the basic syngas production concept of VTT, which is based on steam–oxygen gasification at below 0.4 MPa pressure and 900 °C temperature followed by filtration at ca. 550 °C and catalytic reforming of tars and hydrocarbon gases in a two-stage reformer.

The gasifier operation was steady and a very high carbon conversion of 98.5–99% was reached with all three feedstocks. Raw gas tar contents were reasonably low due to the catalytic effects of the used bed material containing calcium. No signs of bed sintering or ash deposits were found from the bottom ash or from the reactor wall when inspected after the test run. Operation of the filter unit at a 530–560 °C temperature window was smooth and there were no signs of increasing pressure drop. The filter unit removed practically all particulates and alkali metals and over 90% of chlorine from the gas, and thus protected the catalytic reformer unit rather well. The operation of the reformer was also straightforward and the catalyst activity remained constant throughout the test run. The operation temperature could be controlled easily by changing the oxygen feed rates. All C_2-hydrocarbon gases, over 98% of tars and 92–99% of benzene were decomposed in the reformer, whereas the conversion of methane and ammonia was lower. There were no signs of increasing pressure drop in the reformer. In addition, the visual inspection made after the test run showed that both the monoliths of the pre-reformer and the granular catalyst of the final fixed bed were practically free of soot or ash deposits.

Follow-up process development work was later focused on further improvement of the reformer performance. This was accomplished by changing the pre-reformer type from monolith to fixed-bed and by enlarging the volume of the final nickel catalyst bed.

Acknowledgements

This work was financially supported by the Finnish Funding Agency for Technology and Innovation (Tekes) (grant no. 40441/11) through the 2G-Biofuels 2020 project.

References

[1] E. Kurkela Girio, J. Kiel, R.K. Lankhorst, Longer Term R&D Needs and Priorities on Bioenergy, EERA-EIBI Workshop Report, EERA European Energy Research Alliance Bioenergy, Brussels, 2013. (47 p. http://setis.ec.europa.eu/system/files/EERA_EIBI_WORKSHOP_Report.pd).
[2] M. Nieminen, E. Kurkela, J. Palonen, Biomass and waste gasification and gas co-firing in pulverised coal-fired boilers, Proc. of the 6th European Gasification Conference, Institution of Chemical Engineers, Brighton, UK, May 10–12 2004.
[3] S. Kern, C. Pfeifer, H. Hofbauer, Gasification of wood in a dual fluidized bed gasifier: Influence of fuel feeding on process performance, Chem. Eng. Sci. 90 (2013) 284–298, http://dx.doi.org/10.1016/j.ces.2012.12.044.
[4] M. Hedenskog, Gasification of forest residues in a large demonstration scale — The GoBiGas-project, SGC Int. Seminar on Gasification, Malmo, SwedenOct. 15–16, 2014. (http://conference.sgc.se/ckfinder/userfiles/files/2_1_%20Malin%20Hedenskog.pdf).
[5] A.G. Buekens, J.G. Schoeters, European experience in the pyrolysis and gasification of solid wastes, Conserv. Recycl. 9 (1986) 253–269, http://dx.doi.org/10.1016/0361-3658(86)90016-0 (ISSN 0361–3658).
[6] R.J. Evans, R.A. Knight, M. Onischak, S.P. Babu, Development of biomass gasification to produce substitute fuels, Pacific Northwest Lab, Technical Report, PNL-65181988.http://dx.doi.org/10.2172/5206147.
[7] U. Femmer, J. Lambertz, K.A. Theis, Gasification of Brown Coal for the Generation of Synthesis Gas, United States: American Institute of Chemical Engineers, New York, NY, 1986.
[8] J. Koljonen, E. Kurkela, C. Wilen, Peat based HTW-plant at Oulu, Bioresour. Technol. 46 (1993) 95–101.
[9] E. Kurkela, J. Koljonen, Experiences in the operation of the HTW process at the peat ammonia plant of Kemira Oy, in: M. Korhonen (Ed.), ,VTT Symposium 107, Low grade fuels, Helsinki, 12–16 June 1989, vol. 1 1990, pp. 361–372.
[10] E. Kurkela, P. Ståhlberg, Air gasification of peat, wood and brown coal in a pressurized fluidized-bed reactor. I. Carbon conversion, gas yields and tar formation, Fuel Process. Technol. 31 (1992) 1–21, http://dx.doi.org/10.1016/0378-3820(92)90038-R.
[11] E. Kurkela, M. Kurkela, A. Moilanen, 2006, in: A.V. Bridgwater, D.G.B. Boocock (Eds.), Science in Thermal and Chemical Biomass Conversion, vol. 1, CPL Press 2006, pp. 662–676 (Science in Thermal and Chemical Biomass Conversion. Vancouver Island, Canada, 30 Aug.–2 Sept. 2004).
[12] P. McKeough, E. Kurkela, Process evaluations and design studies in the UCG project 2004–2007, Espoo, VTT. 45 p. VTT Tiedotteita — Research Notes 2434, , 2008, ISBN 978-951-38-7209-0. (978-951-38-7210-6).
[13] P. McKeough, K. Saviharju, Enhancing production of energy power and fuels in conjunction with chemical recovery and simultaneously reducing green-house gas emissions, International Chemical Recovery Conference. Quebec, Canada, May 9–June 1, 2007.
[14] I. Hannula, E. Kurkela, Liquid transportation fuels via large-scale fluidised-bed gasification of lignocellulosic biomass. Espoo, VTT. 114 p. + app. 3 p. VTT Technology 91, 2013. (http://www.vtt.fi/inf/pdf/technology/2013/T91.pdf).
[15] P. McKeough, E. Kurkela, Detailed comparison of efficiencies and costs of producing FT liquids, methanol, SNG and hydrogen from biomass, 15th European Biomass Conference, Berlin, Germany, May 7–11, 2007.
[16] E. Kurkela, M. Kurkela, I. Hiltunen, The effects of wood particle size and different process variables on the performance of steam–oxygen blown circulating fluidized-bed gasifier, Environmental Progress and Sustainable Energy, Am. Inst. Chem. Eng. Environ Prog. 33 (2014) (2014) 681–687, http://dx.doi.org/10.1002/ep.12003.
[17] P. Simell, I. Hannula, S. Tuomi, M. Nieminen, E. Kurkela, I. Hiltunen, N. Kaisalo, J. Kihlman, Clean syngas from biomass-process development and concept assessment, Biomass Convers. Bioref. 4 (2014) 357–370, http://dx.doi.org/10.1007/s13399-014-0121-y.
[18] E. Kurkela, P. Ståhlberg, J. Laatikainen, Pressurized fluidized-bed gasification experiments with wood, peat and coal at VTT in 1991–1992, Part 1. Test facilities and gasification experiments with sawdust, VTT Publications, Espoo, VTT, 1993. 55.
[19] P. Simell, J.B. Bredenberg, Catalytic purification of tarry fuel gas, Fuel 69 (1990) 1219–1225.
[20] N. Kaisalo, J. Kihlman, I. Hannula, P. Simell, Reforming solutions for biomass-derived gasification gas: experimental results and concept assessment, Fuel 147 (2015) 208–220, http://dx.doi.org/10.1016/j.fuel.2015.01.056.
[21] P. Simell, E. Kurkela, Method for the purification of gasification gas. Pat. EP1404785 B1, publication date 3 Jan. 2007, application number EP2002743308A, application date 20 June 2002, priority EP2002743308A.
[22] P. Simell, E. Kurkela, I. Hiltunen, S. Toppinen, I. Eilos, Method of reforming gasification gas, WO/2013/030463.
[23] J. Neeft, et al., Tar guideline. A standard method for measurement of tars and particles in biomass producer gases, 12th Eur. Conf. and Technology Exhibition on Biomass for Energy, Industry and Climate Protection, Amsterdam, NL June 17–21 2002, pp. 469–472.
[24] E. Kurkela, P. Ståhlberg, Air gasification of peat, wood and brown coal in a pressurized fluidized-bed reactor. 2. Formation of nitrogen compounds, Fuel Process. Technol. 31 (1991) 23–32.
[25] J. Leppälahti, E. Kurkela, The behaviour of nitrogen compounds and tars in fluidized-bed air gasification of peat, Fuel 70 (1991) 491–497.
[26] R.R. Rhinehart, R. Felder, J.K. Ferrel, Dynamic modelling of a pilot-scale fluidized-bed coal gasification reactor, Ind. Eng. Chem. Res. 26 (1987) 738–745.
[27] J. Laatikainen-Luntama, E. Kurkela, Air-blown CFB gasification of forest residues, demolition wood and crushed wheat straw pellets, manuscript submitted for publication, 22nd International Conference on Fluidized Bed Conversion, June 2015 (Turku, Finland).
[28] E. Kurkela, Formation and removal of biomass-derived contaminants in fluidized-bed gasification processes, VTT Publications, Espoo, VTT 1996, p. 47.
[29] E. Kurkela, P. Ståhlberg, J. Laatikainen, M. Nieminen, Removal of particulates and alkali metals from the product gas of pressurized fluidized-bed gasifier, Proc. Int. Filtration & Separation Conf. FILTECH EUROPA 91, Karlsruhe, DE, 15–17 Oct, Filtration Society 1991, pp. 449–467.
[30] J. Hepola, P. Simell, Sulphur poisoning of nickel-based hot gas cleaning catalysts in synthetic gasification gas. I. Effect of different process parameters, Appl. Catal. B Environ. 14 (1997) 287–303.
[31] J. Hepola, P. Simell, Sulphur poisoning of nickel-based hot gas cleaning catalysts in synthetic gasification gas. II. Chemisorption of hydrogen sulphide, Appl. Catal. B Environ. 14 (1997) 305–321.